



室蘭工業大学

学術資源アーカイブ

Muroran Institute of Technology Academic Resources Archive



CHARACTERISTICS IN AN RF  
SUPERCONDUCTING QUANTUM  
INTERFERENCE DEVICE AS A FUNCTION OF  
APPLIED MAGNETIC FLUX : SYSTEMATIC  
CALCULATIONS I

|       |                                                                                                                          |
|-------|--------------------------------------------------------------------------------------------------------------------------|
| メタデータ | 言語: eng<br>出版者: 室蘭工業大学<br>公開日: 2014-03-04<br>キーワード (Ja):<br>キーワード (En):<br>作成者: 青地, 強志, 戎, 修二, 永田, 正一<br>メールアドレス:<br>所属: |
| URL   | <a href="http://hdl.handle.net/10258/590">http://hdl.handle.net/10258/590</a>                                            |

# CHARACTERISTICS IN AN RF SUPERCONDUCTING QUANTUM INTERFERENCE DEVICE AS A FUNCTION OF APPLIED MAGNETIC FLUX : SYSTEMATIC CALCULATIONS ?

|                              |                                                                               |
|------------------------------|-------------------------------------------------------------------------------|
| 著者                           | AOCHI Tsuyoshi, EBISU Shuji, NAGATA Shoichi                                   |
| journal or publication title | Memoirs of the Muroran Institute of Technology. Science and engineering       |
| volume                       | 42                                                                            |
| page range                   | 33-44                                                                         |
| year                         | 1992-11                                                                       |
| URL                          | <a href="http://hdl.handle.net/10258/590">http://hdl.handle.net/10258/590</a> |

# CHARACTERISTICS IN AN RF SUPERCONDUCTING QUANTUM INTERFERENCE DEVICE AS A FUNCTION OF APPLIED MAGNETIC FLUX : SYSTEMATIC CALCULATIONS I

Tsuyoshi AOCHI, Shuji EBISU and Shoichi NAGATA

## Abstract

There has been a lot of discussion of characteristics in superconducting quantum interference device (SQUID). However, much less information is available on systematic calculations of these behavior. In this report, we describe various features in a superconducting ring having one Josephson junction. Systematic computer calculations of static behavior of the  $\mathcal{rf}$  - SQUID have been carried out. The characteristic features depend strongly on a parameter  $\beta = (2\pi LI_0) / \Phi_0$ , where  $I_0$  is a critical current of the junction,  $L$  is a self - inductance of the ring and  $\Phi_0$  is the flux quantum. In the regime  $\beta > 1$ , the quantum states are discrete and the transitions between the quantum states are irreversible. The present work is focused on the correspondence between energy of the system and the characteristics in the  $\mathcal{rf}$  - SQUID over the range of  $\beta = 0.20$  to  $2\pi$ . The results of the calculations are shown in the following No. 2 paper.

## 1. Introduction

The superconducting quantum interference device (SQUID) is originated from the epoch - making theoretical prediction of the Cooper pairs tunneling between two superconductors.<sup>1)</sup> We will describe here the details of the physical bases and the numerical calculations for the SQUID.

The SQUID has been investigated from various viewpoints and by various kinds of experimental techniques since the first observation by Jaklevic et al. in 1964.<sup>2-4)</sup> These subjects represent some of the purest and most fundamental aspects of the superconductivity.<sup>5-9)</sup>

However, much less information is available on systematic calculations of the characteristics of the SQUID. The present work is concerned with systematic computer calculations of the static behavior of the  $\mathcal{rf}$  - SQUID, which contains one ideal Josephson junction in the superconducting ring.

The SQUIDS are based on the two physical pillars. The first is fluxoid quantization and the second is Josephson effect. Figure 1 shows a superconducting ring with a single Josephson weak link. We shall make the simplification that the ideal Josephson junction area is small enough for the current density to be uniform, and that it never contains a significant fraction of a flux quantum. The internal magnetic flux  $\Phi$  passing through the ring includes the magnetic flux  $LI_s$  gener-

ated by the current  $I_s$  circulating in the ring, where  $L$  is the self – inductance of the ring. As shown in Fig. 1, the internal flux  $\Phi$  threading the ring is then related to the applied flux  $\Phi_x$  by

$$\Phi = \Phi_x - LI_s,$$

where  $\Phi_x$  is the applied flux intercepted by the ring, and  $LI_s$  is the screening flux generated by the induced supercurrent.

In the present paper, many physical quantities have been calculated as a function of applied magnetic flux  $\Phi_x$ . Their behavior depends on the dimensionless parameter  $\beta = (2\pi LI_0) / \Phi_0$ , where  $I_0$  is the critical current of the junction and  $\Phi_0$  is the flux quantum. For  $\beta < 1$ ,  $\Phi$  is a single – valued function of  $\Phi_x$ , whereas in the regime  $\beta > 1$ , it is three – valued around half integer values of  $\Phi_x$ . Then hysteresis appears, for transitions in increasing and decreasing field occur at different  $\Phi_x$  values. Namely the quantum states are discrete and the transitions between

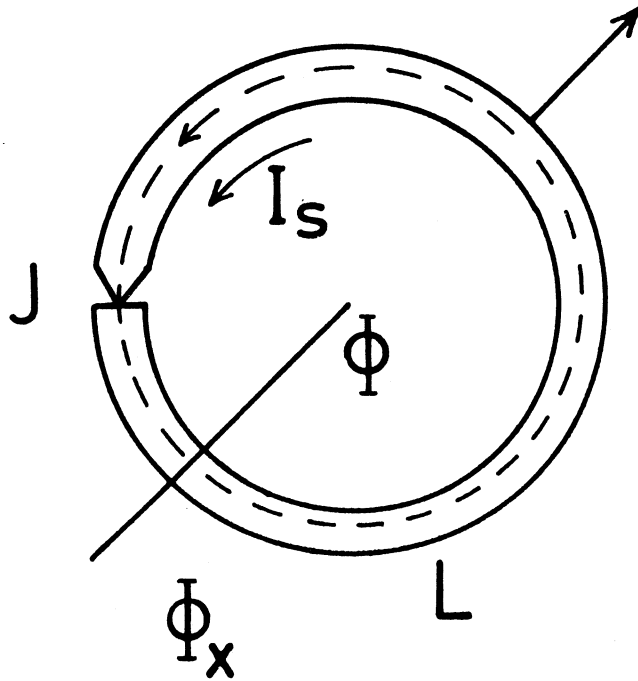


**Fig. 1** Superconducting ring with a ideal Josephson junction denoted by  $J$ . The contour used for integration is shown by the broken line. Internal magnetic flux  $\Phi$ , circulating current  $I_s$ , self – inductance  $L$  and applied magnetic flux  $\Phi_x$  are related by  $\Phi = \Phi_x - LI_s$ . Typical values are  $L = 5\text{nH}$ , and  $I_0 = 1\ \mu\text{A}$ . The junction resistance in the normal state is  $R = 10\ \Omega$ , and the diameter of the ring is about 2mm.

the quantum states are irreversible.

Most practical  $rf$  – SQUIDs have typical values of  $L \sim 5 \times 10^{-10}$  H,  $I_0 \sim 1 \times 10^{-6}$  A ; hence the magnitude of  $\beta$  is about 1.50. Our numerical calculations have been carried out for values of  $\beta$  from 0.20 to  $2\pi$ .

We emphasize the correspondence between the energy of the ring and the various characteristics in the  $rf$  – SQUID. For  $\beta > 1$ , when the applied magnetic flux  $\Phi_x$  is increased, the potential energy barrier preventing transition from the initial fluxoid quantum state to an adjacent one decreases. Actually, the transition occurs as the energy barrier vanishes at a critical value of  $\Phi_x$ .

In section 2 the fluxoid quantization, the Josephson tunneling and the energy of the system are briefly reviewed in order to recall their physical meaning and to define physical quantities for the following discussion.

## 2. Basic Equations

### 2.1 Fluxoid quantization

#### 2.1.1 Bohr – Sommerfeld quantum condition

A closed line integral of the canonical momentum along a path in a superconducting ring can be derived in the presence of a magnetic field. Then the Bohr – Sommerfeld quantum condition gives the fluxoid quantization, as follows :

$$\oint \mathbf{p} \cdot d\mathbf{l} = nh,$$

$$\mathbf{p} = m^* \mathbf{v} + e^* \mathbf{A} \quad (e^* < 0),$$

where  $\mathbf{p}$  is the canonical momentum of a Cooper pair ( $m^* = 2m$ ,  $e^* = 2e$ ),  $\mathbf{A}$  is the vector potential and  $n$  is an integer. If the superconducting ring is sufficiently thick in comparison to the penetration depth then the contribution  $\int m^* \mathbf{v} \cdot d\mathbf{l}$  for the supercurrent vanishes except in the Josephson junction. The dashed line in Fig. 1 represents the integration path. Hence the integral can be written as

$$(1/e^*) \oint \mathbf{p} \cdot d\mathbf{l} = [m^*/(\rho^* e^{*2})] \int_{\text{junction}} \mathbf{j} \cdot d\mathbf{l} + \int_{\text{surface}} \mathbf{B} \cdot d\mathbf{S},$$

which is equal to  $n(h/e^*) = n(h/2e) = n\Phi_0$ . Here  $\mathbf{j}$  is the current density given by  $(\rho^* e^* \mathbf{v})$ ,  $\rho^*$  being the number of the Cooper pair per unit volume. The enclosed flux will be called internal magnetic flux and denoted by  $\Phi$  and the flux quantum is defined to be  $\Phi_0 (= h/2e)$ .

For simplicity we assume that the Josephson junction is sufficiently small in area. Hence we in-

produce a following definition of phase difference across the junction  $\theta$  :

$$\begin{aligned}\theta &\equiv - [m^* / (e^* \rho^* \hbar)] \int_{\text{junction}} j \cdot dl, \\ &= 2\pi [\Phi / \Phi_0 + n].\end{aligned}$$

The minus sign indicates that the direction of current  $j$  is opposite to that of the increase in  $\Phi$ , as can be seen in Fig. 1.

### 2.1.2 Ginzburg – Landau viewpoint

The order parameter is a complex quantity as

$$\Psi = |\Psi(x, y, z)| \exp[i\phi(x, y, z)],$$

where the amplitude is  $|\Psi(x, y, z)| = \sqrt{\rho^*}$  and  $\phi(x, y, z)$  is the phase. A relationship between the current density flowing in the superconductor and the order parameter in the presence of a magnetic field is given by<sup>5)</sup>

$$j = [e^* \hbar / (2m^* i)] \{ \Psi^* \nabla \Psi - \Psi \nabla \Psi^* \} - (e^{*2} / m^*) A |\Psi|^2.$$

Substituting  $\Psi$  into this equation, we get

$$\nabla \phi = (e^* / \hbar) A + [m^* / (e^* \rho^* \hbar)] j.$$

From the viewpoint of GL theory, the fluxoid quantization is based on the existence of a single – valued complex superconducting order parameter  $\Psi$ . This requires that the phase  $\phi(x, y, z)$  must change by an integral multiple of  $2\pi$  when a complete close circuit has been covered.

$$\begin{aligned}2\pi n &= (e^* / \hbar) \int_{\text{surface}} B \cdot dS + [m^* / (e^* \rho^* \hbar)] \int_{\text{junction}} j \cdot dl, \\ &= (e^* / \hbar) \int_{\text{surface}} B \cdot dS + \theta.\end{aligned}$$

Then, the value of the phase difference  $\theta$  and defined by

$$\begin{aligned}\theta &\equiv - [m^* / (e^* \rho^* \hbar)] \int_{\text{junction}} j \cdot dl, \\ &= 2\pi [\Phi / \Phi_0 + n].\end{aligned}$$

## 2.2 Josephson current

The superconducting current  $I$  across the junction shown in Fig. 1 depends on the phase differ-

ence  $\theta$  as<sup>10)</sup>

$$I = I_0 \sin \{ \theta (0) + e^* Vt / \hbar \}$$

where  $I_0$  is the maximum zero – voltage current that can be passed by the junction and  $V$  is a constant  $dc$  bias voltage. With no bias voltage (the  $dc$  Josephson effect) a  $dc$  current will flow across the junction with a value between  $I_0$  and  $-I_0$  according to the value of the phase difference  $\theta$ . This phase difference  $\theta$  adjusts to the current  $I$ , according to the above Josephson relation. If a current greater than  $I_0$  is passed through the junction, a voltage appears across it.

### 2.3 Energy of the system

If the current through the junction is varying with time, the phase difference  $\theta$  must also be changing with time, and it can be shown that a voltage  $V$  is developed across it. This voltage is related to the time rate of  $\theta$  by<sup>10)</sup>

$$\frac{d\theta}{dt} = \frac{2e}{\hbar} V.$$

Consider a junction through which a constant current  $I_s$  is flowing, the current having been raised from zero to this value over a time  $t$ . During the time the current is increasing, the rate of change of current  $dI / dt$  corresponds to a voltage  $V$  across the junction. Therefore, power  $IV$  is being delivered to it and work,  $dE_J = IVdt$ , is performed in setting up the current and the consequent phase difference. The value of  $dE_J$  is the increase in energy of the junction due to the passage of a current through it and  $dE_J$  is given by<sup>10)</sup>

$$\begin{aligned} dE_J &= IVdt, \\ &= (I_0\hbar) / (2e) \sin \theta \frac{d\theta}{dt} dt. \end{aligned}$$

Then, we obtain the junction coupling energy  $E_J$  which depends on the phase difference, as

$$\begin{aligned} E_J &= (I_0\hbar) / (2e) [1 - \cos \theta], \\ &\equiv - E_0 \cos \theta + \text{constant}. \end{aligned}$$

Provided  $E_J$  is large compared with the thermal fluctuation energy  $k_B T$ , phase coherence extends across the barrier and a supercurrent can be passed through up to the critical current  $I_0$ .

On the other hand if the current  $I$  goes through the superconducting ring, the magnetic energy of the current flowing in the inductance  $L$  is  $(1 / 2) LI^2$ . The energy of the system of the supercon-

ducting ring is then expressed by two terms,<sup>11)</sup>

$$\begin{aligned}
 U &= \frac{1}{2} L I_s^2 - E_0 \cos \theta, \\
 &= \left( \frac{1}{2L} \right) (\Phi - \Phi_x)^2 - E_0 \cos \left( \frac{2\pi \Phi}{\Phi_0} \right),
 \end{aligned}$$

where the first term is the magnetic energy  $E_m$  associated with a current and the second is the junction coupling energy  $E_J$ . Here the electro-static Coulomb energy associated with any difference in charge density between the two sides of the barrier is neglected. The extra amount of constant energy is also assumed to be zero.

## 2.4 Basic equations

The basic equations are summarized and are described below. The main characteristics of the rf – SQUID are the behaviors of the internal flux  $\Phi$  and of the screening circulating current  $I_s$  as a function of the external flux  $\Phi_x$ . They are derived from the next equations,

$$\Phi = \Phi_x - L I_s, \quad (1)$$

$$\theta = 2\pi [\Phi / \Phi_0 + n], \quad (2)$$

$$I_s = I_0 \sin \theta. \quad (3)$$

Equations (1), (2) and (3) are linked equations for the three unknown quantities  $\Phi$ ,  $I_s$  and  $\theta$  in terms of the applied flux  $\Phi_x$ . Here we introduce dimensionless parameter  $\beta$ , defined as

$$\beta = (2\pi L I_0) / \Phi_0, \quad (4)$$

where  $\beta$  depends on the value of  $L I_0$ . The limiting forms of the equations are  $\Phi = \Phi_x$  for  $L I_0 = 0$ , which corresponds to an open ring, and complete flux quantization  $\Phi = n \Phi_0$  for  $L I_0 \gg \Phi_0$ , which corresponds to a closed ring with no weak link. Making the substitution of eqs. (2) and (3) into eq. (1), we get a next relation,

$$\Phi = \Phi_x - L I_0 \sin (2\pi \Phi / \Phi_0). \quad (5)$$

Substituting eqs. (1) and (2) into eq. (3) gives

$$I_s = I_0 \sin (2\pi \Phi / \Phi_0). \quad (6)$$

For the ring with a junction the energy of the system is given by

$$U = \left(\frac{1}{2L}\right) (\Phi - \Phi_x)^2 - E_0 \cos\left(\frac{2\pi\Phi}{\Phi_0}\right). \quad (7)$$

### 3. Numerical Computer Calculations for the Characteristics in *rf*– SQUID

#### 3.1 The system energy $U(\Phi, \Phi_x)$

The system energy  $U$ , normalized by  $(\Phi_0^2 / 2L)$ , is written as

$$U / (\Phi_0^2 / 2L) = (\Phi / \Phi_0 - \Phi_x / \Phi_0)^2 - \beta / (2\pi^2) \cos(2\pi\Phi / \Phi_0). \quad (8)$$

The energy  $U(\Phi, \Phi_x)$  of the system given by eq. (8) is calculated. Figures 2 to 11 show the results of  $U(\Phi, \Phi_x)$  for various values of parameter  $\beta$ . Using partial derivative of  $U(\Phi, \Phi_x)$  with respect to  $\Phi$ , the condition at the local minimums of  $U(\Phi, \Phi_x)$  is

$$\frac{\partial U(\Phi, \Phi_x)}{\partial \Phi} = 0, \quad (9)$$

which leads to the next equation :

$$\Phi = \Phi_x - LI_0 \sin\left(\frac{2\pi\Phi}{\Phi_0}\right). \quad (10)$$

This is exactly the same equation to eq. (5). We can get the following relation :

$$\frac{d\Phi}{d\Phi_x} = \frac{1}{1 + \beta \cos(2\pi\Phi / \Phi_0)}. \quad (11)$$

For  $\beta < 1$ , the denominator of eq. (11) has always positive value and then there are no portions of the curve with negative slope in  $\Phi$ . Therefore,  $\Phi$  is a single – valued function. As a result, the ring has only one stable state whose  $\Phi$  value is obtained by eq. (10) for any value of  $\Phi_x$ . On the other hand, for  $\beta > 1$ ,  $\Phi$  in eq. (10) is three – valued for some parts of the range  $\Phi_x$ . Then meta-stable states can exist. Consequently, hysteresis can occur since the transitions in increasing and decreasing flux occur at different  $\Phi_{xc}$ .

For an example, let explain the behavior of the hysteresis in Fig. 9 in the case of  $\beta = 1.50$ . Figure 9 shows the behavior in the low energy portion of  $U$  for  $\beta = 1.50$  in greater detail. There are two specific inflection points at  $\Phi / \Phi_0 = 0.366$  and  $0.634$  in Fig. 9. When increasing the external flux  $\Phi_x$ , the transition occurs at  $\Phi_{xc} / \Phi_0 = 0.544$ , whereas it takes place at  $\Phi_{xc} / \Phi_0 = 0.456$  when decreasing the flux. Up to flux  $\Phi_{xc}$  the system is maintained in the lower flux side of the potential valley by the central barrier, even if it is in the unstable equilibrium state (see  $\Phi_x = 0.52$  in Fig. 9). Finally the barrier vanishes at  $\Phi_{xc}$  and the transition takes place. During the back process the system change occurs in the inverse order.

The behavior of the system can be understood by considering its trajectory. The essential feature is that the external flux jumps from an initial fluxoid quantum state to the next fluxoid state.

### 3.2 The junction coupling energy $E_J$ vs. external flux $\Phi_x$

The junction coupling energy is

$$E_J = -E_0 \cos(2\pi \Phi / \Phi_0). \quad (12)$$

Using the expressions of  $E_0$  and  $\beta$ , we get the normalized form of  $E_J$

$$E_J / (\Phi_0^2 / 2L) = -[\beta / (2\pi^2)] \cos(2\pi \Phi / \Phi_0). \quad (13)$$

Figures 12 to 17 display the  $E_J$  vs.  $\Phi_x$  for the following values of parameter  $\beta$ : 0.20, 0.50, 1.00, 1.50, 3.00 and  $2\pi$ . The derivative of  $E_J$  with respect to  $\Phi_x$  becomes

$$\frac{dE_J}{d\Phi_x} = \frac{I_0 \sin(2\pi \Phi / \Phi_0)}{1 + \beta \cos(2\pi \Phi / \Phi_0)}. \quad (14)$$

For  $\beta > 1$ , if  $\cos \theta = -1 / \beta$ , the denominator of eq. (14) goes to zero, leading to an infinite slope of  $E_J$  at  $\Phi_{xc}$ .  $\Phi_{xc}$  is given by the next two equations:

$$\Phi_{xc} / \Phi_0 = \Phi / \Phi_0 \pm (\beta / 2\pi) (1 - \beta^{-2})^{1/2}, \quad (15)$$

$$\Phi / \Phi_0 = (1 / 2\pi) \cos^{-1}(-1 / \beta). \quad (16)$$

As an example, in the case  $\beta = 1.50$ , we get two values of  $\Phi_{xc} / \Phi_0$ , namely 0.544 and 0.456, in the range  $0 < \Phi / \Phi_0 < 1$ . These critical values are exactly the same as those obtained from the analysis of the system energy  $U$ , as explained previously. That is, hysteresis occurs since the transitions in increasing and decreasing flux takes place at different  $\Phi_x$  values. These critical values  $\Phi_{xc}$  correspond to the position at which the slope of  $E_J$  takes infinite value.

### 3.3 The magnetic energy $E_m$ vs. external flux $\Phi_x$

The magnetic energy of the ring is

$$E_m = \left(\frac{1}{2L}\right) (\Phi - \Phi_x)^2. \quad (17)$$

The normalized form is

$$E_m / (\Phi_0^2 / 2L) = [\beta / (2\pi)]^2 \sin^2(2\pi \Phi / \Phi_0). \quad (18)$$

Figures 12 to 17 show the  $E_m$  vs.  $\Phi_x$  behavior with parameter  $\beta$  from 0.20 to  $2\pi$ .

The derivative of  $E_m$  with respect to  $\Phi_x$  becomes

$$\frac{dE_m}{d\Phi_x} = \frac{(\beta / L)(\Phi_x - \Phi) \cos(2\pi \Phi / \Phi_0)}{1 + \beta \cos(2\pi \Phi / \Phi_0)}. \quad (19)$$

For  $\beta > 1$ , if  $\cos \theta = -1 / \beta$ , the denominator of eq. (19) goes to zero, leading to an infinite slope of  $E_m$  at  $\Phi_{xc}$ . The value of  $\Phi_{xc}$  is the same as obtained by eqs. (15) and (16).

Hysteresis occurs when the transitions in increasing and decreasing flux take place at different  $\Phi_x$  values. These critical value  $\Phi_{xc}$  corresponds to the position at which the slope of  $E_m$  gives infinite value.

The total energy  $U$ , which is normalized, is also shown in Figs. 12 to 17. The value of  $U$  in these figures corresponds to the maximum or minimum value in Figs 6 to 11

### 3.4 $E_J$ , $E_m$ vs. phase difference $\theta$

The junction coupling energy  $E_J$ , the magnetic energy  $E_m$  and the system energy  $U$  are expressed as a function of the phase difference  $\theta$  as follows :

$$E_J / (\Phi_0^2 / 2L) = - [\beta / (2\pi^2)] \cos \theta, \quad (20)$$

$$E_m / (\Phi_0^2 / 2L) = [\beta / (2\pi)]^2 \sin^2 \theta, \quad (21)$$

$$U / (\Phi_0^2 / 2L) = - [\beta / (2\pi^2)] \cos \theta + [\beta / (2\pi)]^2 \sin^2 \theta, \quad (22)$$

$$= - [\beta / (2\pi^2)] \cos(2\pi \Phi / \Phi_0) + [\beta / (2\pi)]^2 \sin^2(2\pi \Phi / \Phi_0). \quad (23)$$

Equation (23) can be also obtained by making a substitution of eq. (10) into eq. (8). Consequently the physical meaning of eqs. (22) and (23) is that the minimum, the maximum, local minimum or local maximum energies of the superconducting ring are given by eqs. (22) or (23). Figures 18 to 23 show the behavior of these functions for several values of  $\beta$ .

The derivative  $U$  with respect to  $\theta$  gives

$$d[U / (\Phi_0^2 / 2L)] / d\theta = [\beta / (2\pi^2)] \sin \theta [1 + \beta \cos \theta]. \quad (24)$$

When  $\beta < 1$ , the superconducting ring has a minimum energy at  $\theta = 0$  and a maximum energy at  $\theta = \pi$ . On the other hand, when  $\beta > 1$ , the system has a minimum energy at  $\theta = 0$  and a maximum energy at  $\theta = \cos^{-1}(-1 / \beta)$ .

### 3.5 Internal flux $\Phi$ vs. external flux $\Phi_x$

In Fig. 24 to 29, results of calculations for  $\Phi$  versus  $\Phi_x$  relation are shown. These behavior depends on the dimensionless parameter  $\beta = (2\pi LI_0) / \Phi_0$ . Taking the derivatives of  $\Phi$  with re-

spect to  $\Phi_x$ , we can get the following relations using eqs. (5) or (10) :

$$\frac{d\Phi}{d\Phi_x} = \frac{1}{1 + \beta \cos(2\pi\Phi/\Phi_0)}. \quad (25)$$

For  $\beta < 1$ , the denominator of eq. (25) is always positive and then, there are no portions of the curve with negative  $\Phi$  vs.  $\Phi_x$  slope. Namely, the value of  $\Phi$  increases monotonically as a function of  $\Phi_x$ . Therefore,  $\Phi$  is a single-valued function of  $\Phi_x$ . The slope of  $\Phi$  is maximum at  $\Phi_x/\Phi_0 = 1/2$ . On the contrary, for  $\beta > 1$ , the  $\Phi$  vs.  $\Phi_x$  curves have regions of negative slope. The portions with negative slope in these curves are unstable. This point has been already discussed from the viewpoint of the system energy  $U$ . Namely the quantum states are discrete and the transitions between the quantum states are irreversible. Consequently, hysteresis exists when the transitions in increasing and decreasing field occur at different  $\Phi_x$  values.

For  $\beta > 1$ , if  $\cos\theta = -1/\beta$ , the denominator of eq. (25) goes to zero leading to an infinite slope of  $\Phi$  vs.  $\Phi_x$  at  $\Phi_{xc}$ . These values  $\Phi_{xc}$  are given by the two equations (15) and (16). As an example, in the case  $\beta = 1.50$ , values 0.544 and 0.456 for  $\Phi_{xc}/\Phi_0$  correspond to the critical positions of the transitions when  $\Phi_x$  increases or decreases in a range of  $0 < \Phi_x/\Phi_0 < 1$ , respectively. These critical values are exactly the same as those obtained from the analysis for the system energy  $U$ .

When increasing  $\beta$ , the flux ranges of successive hysteresis path overlaps partly as can be seen in Fig. 29. The critical value of  $\beta$  leading to overlap of the hysteresis path is given by the criterion that the critical external flux  $\Phi_{xc}$  of the one fluxoid quantum state reaches zero in the decreasing flux process. Then the critical value of  $\beta_0$  is deduced by the two eqs. (15) and (16), which give the next equation.

$$(1/2\pi) \cos^{-1}(-1/\beta_0) = (\beta_0/2\pi)(1 - \beta_0^{-2})^{1/2}. \quad (26)$$

We can obtain the critical value of  $\beta_0$  by numerical calculation,

$$\beta_0 = 4.6033. \quad (27)$$

### 3.6 Induced flux $LI_s$ vs. external flux $\Phi_x$

In Fig. 24 to 29, results of calculations of  $LI_s$  versus  $\Phi_x$  are shown. The numerical calculations have been made by using eq. (1). The calculated curves depend on the dimensionless parameter  $\beta$ . In these figures the positive or negative sign of  $LI_s$  correspond to the current direction in the ring. By considering eq. (1), the value of  $LI_s$  is obtained by subtracting the value of  $\Phi$  from the diagonal line in the  $\Phi$  vs.  $\Phi_x$  relation. Hence the criterion for hysteresis is derived in

the same way as for the  $\Phi$  vs.  $\Phi_x$  curves. For  $\beta < 1$ ,  $I_s$  is a single – valued functions of  $\Phi_x$ , whereas for  $\beta > 1$ ,  $I_s$  is three – valued in some parts of the  $\Phi_x$  range. Hysteresis appears since the transitions in increasing and decreasing flux occur at different  $\Phi_x$  values. The critical value  $\Phi_{xc}$  corresponds to the position at which the slope of  $I_s$  becomes infinite. These values of  $\Phi_{xc}$  are exactly the same as those obtained by the analysis of the system energy  $U$  as well as the case of  $\Phi$  vs.  $\Phi_x$ .

It should be noticed that the transition does not take place at the maximum value  $I_0$  but at the value  $I_{sc}$  given by

$$I_{sc} = I_0(1 - \beta^{-2})^{1/2} \quad (\beta > 1). \quad (28)$$

For  $\beta = 1.50$ , the critical value of the current  $I_{sc}$  is  $0.745I_0$ . In addition, the screening current has the form  $I_0 \sin(2\pi\Phi / \Phi_0)$ . Then the maximum current appears always at  $\Phi / \Phi_0 = 1/4$ .

### 3.7 Phase difference $\theta$ vs. external flux $\Phi_x$

In Figs. 30 to 35, the values of the phase difference  $\theta$  across the junction as a function of external flux  $\Phi_x$  are shown. Taking the derivatives of  $\theta$  with respect to  $\Phi_x$ , we obtain

$$\frac{d\theta}{d\Phi_x} = \frac{(2\pi / \Phi_0)}{1 + \beta \cos(2\pi\Phi / \Phi_0)}. \quad (29)$$

For  $\beta < 1$ , the denominator of eq. (29) is always positive and there are no portions of the  $\theta$  vs.  $\Phi_x$  curves with negative slope. Therefore,  $\theta$  is a single – valued functions of  $\Phi_x$ . Instead, for  $\beta > 1$ ,  $\theta$  is multi – valued for some parts of the  $\Phi_x$  range. Hysteresis appears since the transitions in increasing and decreasing flux occur at different  $\Phi_x$  values. These critical values  $\Phi_{xc}$  correspond to the position at which the slope of  $\theta$  takes an infinite value.

### 3.8 Fluxoid vs. external flux $\Phi_x$

In Figs. 30 to 35, results of the absolute value of  $|\text{fluxoid} / \Phi_0|$  are shown as a function of  $\Phi_x$ . The applied flux  $\Phi_x$  is able to drive the transition from one fluxoid quantum state to another successive quantum state. From eq. (2),  $|\text{fluxoid} / \Phi_0|$  is integer  $n$  which is expressed as

$$|\text{fluxoid} / \Phi_0| = n = (\theta / 2\pi) - (\Phi / \Phi_0). \quad (30)$$

The derivative of  $n$  is

$$\begin{aligned} \frac{dn}{d\Phi_x} &= (1 / 2\pi) \frac{d\theta}{d\Phi_x} - (1 / \Phi_0) \frac{d\Phi}{d\Phi_x}, \\ &= \frac{1}{1 + \beta \cos(2\pi\Phi / \Phi_0)} [(1 / \Phi_0) - (1 / \Phi_0)]. \end{aligned} \quad (31)$$

The derivative can have a non zero value only if  $\cos \theta = -1 / \beta$ , which corresponds to the transitions between two fluxoid quantum states. These critical values have also the same magnitudes as those given by the analysis of the system energy  $U$ . The derivative of eq. (31) is zero if  $\cos \theta \neq -1 / \beta$ , which means for  $n$  to be constant.

For  $\beta < 1$ , the fluxoid can change at  $\Phi_x / \Phi_0 = 1 / 2$ : the system energy reaches its maximum value corresponding to  $\theta = \pi$  and one flux quantum can enter into the ring.

### References

- 1) B. D. Josephson : Phys. Lett. *1*, (1962) 251.
- 2) R. C. Jaklevic, J. Lambe, A. H. Silver and J. E. Mercereau : Phys. Rev. Lett. *12*, (1964) 159.
- 3) A. H. Silver and J. E. Zimmerman : Phys. Rev. *157*, (1967) 317.
- 4) J. E. Zimmerman P. Thiene and J. T. Harding : J. Appl. Phys. *41*, (1970) 1572.
- 5) L. Solymar : *Superconductive Tunnelling and Applications* (Chapman and Hall, London 1972) p. 217.
- 6) M. Tinkham : *Introduction to Superconductivity* (McGraw – Hill, 1975) p. 192.
- 7) T. Van Duzer and C. W. Turner : *Principles of Superconductive Devices and Circuits* (Elsevier, New York, Oxford, 1981) p. 165.
- 8) A. Barone and G. Paterno : *Physics and Applications of the Josephson Effect* (John Wiley & Sons, 1982) p. 383.
- 9) E. Burstein and S. Lundqvist : *Tunneling Phenomena in Solids* (Plenum Press, New York, 1969) p. 477.
- 10) B. D. Josephson : Adv. Phys. *14*, (1965) 419.
- 11) A. M. Goldman, P. J. Kreisman and D. J. Scalapino : Phys. Rev. Lett. *15*, (1965) 495.

### Figure Captions

Figures of the numerical calculations of the characteristics in the  $rf$  – SQUID and the figure captions are given in the following paper.